Chemical Science

Accepted Manuscript

This article can be cited before page numbers have been issued, to do this please use: L. Jing, Y. Chang, H. Li, B. Lv, G. Yang, Z. Li and B. Yang, *Chem. Sci.*, 2026, DOI: 10.1039/D5SC09220E.

ROYAL SOCIETY OF CHEMISTRY

rsc.li/chemical-science

View Article Online
DOI: 10.1039/D5SC09220E

ARTICLE

Rational Guest Selection: A General Principle for Stabilizing Multi-Component Luminescent Materials

Received 00th January 20xx,
Accepted 00th January 20xx

DOI: 10.1039/x0xx00000x

Li-Ke Jing,[†a] Yue-Yue Chang,[†b] He Li,[c] Biao Lv,[a] Guan-Yu Yang,[a] Zhan-Ting Li,[d] and Bo Yang*[a]

The practical deployment of multi-component luminescent materials is universally hampered by the photodegradation of organic guests, a fundamental challenge that conventional host-centric designs struggle to overcome. Herein, we propose a paradigm-shifting strategy termed "Rational Guest Selection," which elevates the intrinsic molecular photostability of emissive guests to a primary design criterion, equal in importance to emission color. This principle is rigorously validated using the first metal-organic framework constructed from europium ions and pillar[6]arene (**Eu-P6MOF**) as a model host. While a white-light-emitting composite was initially achieved by co-encapsulating Coumarin 6 and Coumarin 1, its emission color shifted significantly under illumination due to the degradation of Coumarin 1. By applying our principle—rationally replacing the unstable Coumarin 1 with the robust perylene dye—we constructed a stable white-light-emitting composite. The generality of this approach is demonstrated by its success in a low-toxicity ethanol solvent. Mechanistic studies reveal that the rigid MOF pores suppress molecular motions associated with non-radiative decay and photodegradation, with the efficacy of this stabilization being dictated by the guest's innate structural rigidity. The "Rational Guest Selection" principle established here provides a universal blueprint for designing durable multi-component functional materials, transcending specific hosts and applications.

Introduction

The integration of distinct luminophores into a single matrix to create multi-component luminescent materials presents a highly attractive route for developing advanced devices, ranging from high-performance white-light-emitting diodes and full-color displays to chemical sensors.[1-4] Metal-organic frameworks (MOFs), with their structurally tunable and well-defined pores, serve as ideal host matrices for precisely constructing such multi-component systems via the encapsulation of organic dye molecules.[5-8] MOF-based host–guest systems exhibit high versatility for constructing tunable luminescent materials and regulating their photophysical properties.[9,10] However, the practical application of these host-guest materials is universally hampered by a persistent and critical challenge: the irreversible photodegradation of organic guests, particularly the indispensable blue emitters, leading to drifts in luminescent color and overall performance decay.[11-14] Conventional research strategies have primarily focused on optimizing the stability and luminescence properties of the host framework,[15-21] somewhat overlooking a more fundamental issue—the intrinsic photochemical instability of the guest molecules themselves.[22-24] Consequently, a paradigm shift is urgently needed in this field: moving from passively relying on the innate stability of guests to proactively selecting guests with high stability at the molecular design level.

To realize this shift, we propose a universal design principle: Rational Guest Selection. The core of this principle is to treat the photostability of guest molecules as a critical design parameter, on par with emission color and energy transfer efficiency.[25, 26] To validate this principle, an ideal model system that can clearly manifest the impact of guest stability and allows for precise structural elucidation is required. Pillar[n]arenes, as an emerging class of macrocyclic hosts with rigid backbones and electron-rich cavities, are ideal building blocks for such a model platform, facilitating the construction of robust porous frameworks and promoting weak interactions with aromatic guests.[27-33]

Based on this rationale, we designed and synthesized the first crystalline framework based on carboxylate-decorated pillar[6]arene and europium ions, denoted as **Eu-P6MOF**. This material features large one-dimensional channels, providing a unique microenvironment for investigating host-guest interactions. We initially achieved white-light emission by encapsulating green-emitting Coumarin 6 and blue-emitting Coumarin 1 within its pores. However, as anticipated, this system exhibited significant chromaticity shifts due to the

[a.] *College of Chemistry, Zhengzhou University, 100 Kexue Street, Zhengzhou, Henan 450001, China. E-mail: yangbohy@zzu.edu.cn*
[b.] *Department of Criminal Science and Technology, Henan Police College, Zhengzhou, Henan 450046, China.*
[c.] *Innovation Team of Optical Functional Molecular, Devices, Inner Mongolia Key Laboratory for the Natural Products Chemistry and Functional Molecular Synthesis, College of Chemistry and Materials Science, Inner Mongolia Minzu University, Tongliao 028000, China.*
[d.] *State Key Laboratory of Organometallic Chemistry, Shanghai Institute of Organic Chemistry, Chinese Academy of Sciences, University of Chinese Academy of Sciences, Shanghai, 200032, China.*
† L. K. JIng and Y. Y. Zhang contributed equally to this work.
Supplementary Information available: [details of any supplementary information available should be included here]. See DOI: 10.1039/x0xx00000x

degradation of Coumarin 1, precisely illustrating the inherent drawback of neglecting guest stability.

This outcome, far from being a failure, provided a crucial opportunity to validate our principle. Through rational selection, we replaced Coumarin 1 with perylene, a dye possessing a rigid fused-ring structure and exceptional photostability,[20] successfully constructing a white-light-emitting composite with remarkable stability under prolonged illumination. More importantly, this strategy proved equally effective in a low-toxicity ethanol solvent,[34] underscoring its generality. This work not only reports the first family of lanthanide-pillararene frameworks (**Eu-P6MOF**) but, more significantly, establishes a universal design principle that transcends specific material systems: the macroscopic stability of a material can be decisively engineered by rationally selecting guest molecules with intrinsic stability. The principle of "Rational Guest Selection" provides a clear blueprint for addressing the long-standing stability challenge in multi-component functional materials, pushing the research paradigm from traditional "host engineering" towards a new stage of comprehensive "host-guest synergistic design".

Results and discussion

Design and Structural Characterization of a Novel Pillararene-Based MOF Host

To provide an ideal platform for validating our principle, we designed and synthesized the first crystalline framework based on a tetracarboxylate-functionalized pillar[6]arene ligand (H_8P6A, Figure 1a) and europium ions, denoted as **Eu-P6MOF**. Single-crystal X-ray diffraction analysis unambiguously reveals its intricate and highly porous architecture. The framework is constructed from a linear pentanuclear heterometallic cluster with a precise K-Eu-Eu-Eu-K sequence (Figure 1b). Each pair of pillar[6]arene ligands coordinates to the central cluster in a distinct V-shaped fashion, giving rise to an overall zigzag (or N-type) supramolecular assembly (Figure 1c). The structure exhibits large, well-defined one-dimensional channels with a diameter of approximately 2.1 nm when viewed along the [100] direction (Figure 1d), providing a unique microenvironment for guest encapsulation. The view down the [001] direction shows the pillar[6]arene cavities in a side-by-side, offset stacking mode (Figure 1e), and the alternating arrangement of metal clusters and organic ligands is clearly observed along the [010] direction (Figure 1f).

The powder X-ray diffraction (PXRD) pattern confirmed the high crystallinity of **Eu-P6MOF** (Figure S1). Chemical stability tests demonstrated that the framework maintained its structural integrity after being immersed in N,N-dimethylformamide (DMF) or ethanol (EtOH) for one day (Figure S2). Thermogravimetric analysis (TGA) indicated high thermal stability, with the framework decomposing only above 350 °C (Figure S3). Elemental mapping analysis verified the homogeneous distribution of C, O, N, Eu, and K throughout the material (Figure S4).

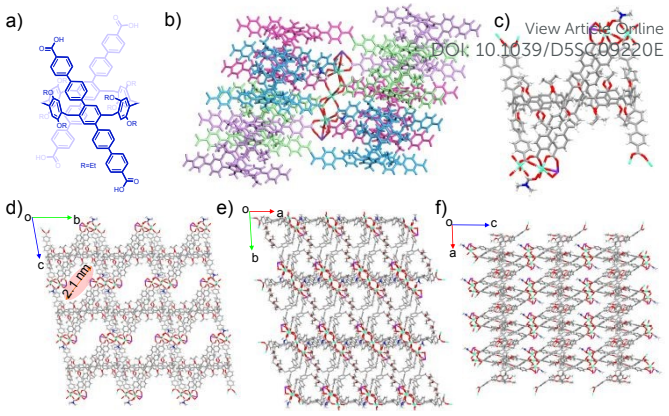

Figure 1. (a) Molecular structure of the tetrabenzoic acid-functionalized pillar[6]arene (H_8P6A) ligand. (b) The linear pentanuclear heterometallic cluster (K–Eu–Eu–Eu–K). (c) The alternating V-shaped arrangement of the pillar[6]arene ligands around the metal chain. (d) The large one-dimensional channels with a diameter of ~2.1 nm in [100] direction. (e) The parallel, offset stacking of the pillar[6]arene macrocycles in [001] direction. (f) The alternating columns of metal clusters and organic ligands in [010] direction.

Successful Construction and Characterization of Host-Guest Composites

With the robust and porous **Eu-P6MOF** host in hand, we proceeded to encapsulate dye molecules. To corroborate the successful and non-destructive incorporation of dyes within the MOF pores rather than mere surface adsorption, we performed dynamic light scattering (DLS) measurements (Figure 2a, Figure S5). The pristine **Eu-P6MOF** exhibited a monomodal hydrodynamic size distribution centered around 170 nm. Notably, after the sequential incorporation of dye molecules (C6: coumarin 6, C1: coumarin 1, perylene) - for both the **Eu-P6MOF-C6-C1** and **Eu-P6MOF-C6-Perylene** composites - the particle size did not decrease but showed a consistent, slight increase. This observation rules out framework fragmentation and is consistent with the dyes residing within the porous framework, providing direct physical evidence for the formation of intact host-guest composites. UV-Vis spectra (Figure 2b, Figure S6) provided additional insight into the host-guest interactions. The slight but discernible shifts in the absorption peaks of the encapsulated dyes (C1 and C6) indicate a change in their micro-environment upon incorporation into the **Eu-P6MOF** pores, likely due to π-π stacking or other weak interactions with the channel walls. Fluorescence titration of the dyes with **Eu-P6MOF** showed gradual quenching of their characteristic emission peaks upon increasing MOF addition, providing further evidence of host–guest interactions (Figures S7–S9). The Brunauer–Emmett–Teller (BET) surface area was calculated to be 9.98 $m^2 g^{-1}$ based on N_2 sorption at 77 K (Figure S10). This apparent limitation, often observed in macrocyclic-based frameworks, does not preclude functionality, as such systems have demonstrated exceptional performance in applications requiring host-guest interactions.[35-37]

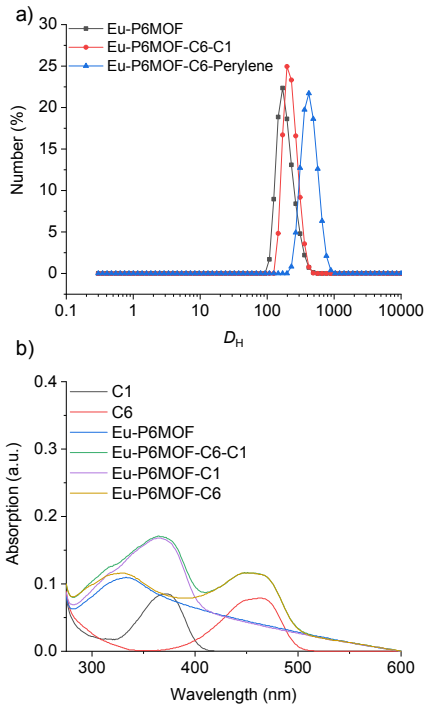

Figure 2. (a) The hydrodynamic diameters (D_H) of the aggregates of **Eu-P6MOF**, **Eu-P6MOF-C6-C1** and **Eu-P6MOF-C6-Perylene** in DMF at 25 ℃. (b) The UV-Vis spectra of **Eu-P6MOF**, C6, C1, **Eu-P6MOF-C1**, **Eu-P6MOF-C6** and **Eu-P6MOF-C6-C1** in DMF.

Achieving White Light and Identifying the Instability Bottlenecks

The fluorescence behavior of **Eu-P6MOF** was first investigated in solvents with different polarities to evaluate potential solvent effects (Figure S11). In all cases, the characteristic Eu^{3+} emission band ($^5D_0 \rightarrow {}^7F_2$) remained centered at ~616 nm, indicating that the fundamental emissive transition of the Eu centers is largely insensitive to the surrounding solvent environment. To further examine the influence of solvent polarity on the excited state, a Lippert–Mataga analysis was constructed based on the emission maxima in different solvents. The resulting plot exhibits an essentially zero slope, suggesting that variations in solvent polarity do not lead to measurable stabilization or destabilization of the emissive excited state. Despite the nearly unchanged emission wavelength, noticeable differences in emission intensity were observed among the solvents, which consequently influenced the overall emission color and CIE coordinates of the suspensions. Among the tested solvents, the **Eu-P6MOF** suspension in DMF exhibited the highest emission intensity and the purest red emission (Figure S12). Therefore, DMF was selected as the solvent platform for the subsequent white-light tuning experiments. Under 296 nm excitation, we employed a stepwise and precise dye-loading strategy: titrating green-emitting C6 into the **Eu-P6MOF** suspension progressively shifted the emission from red to yellow-green. Subsequent introduction of blue-emitting C1 compensated the blue component, steering the coordinates toward the white-light region. Ultimately, high-quality white emission (CIE: 0.3337, 0.3346) was achieved after adding 0.5 μg of C1 (Figure 3a, 3c and Table S1). However, this initial success was tempered by the discovery of a critical flaw: the system suffered from significant photodegradation, with CIE coordinates shifting markedly after 24-hour illumination (Figure 3b, 3d and Table S2). Control experiments pinpointed the instability to C1, as both the free dye and its MOF composite showed marked chromaticity shifts, unlike the stable **Eu-P6MOF** and C6 (Figure S13-S17). To further quantify this instability, the fluorescence decay of the C1 emission under continuous irradiation was analyzed. The decay profile could be fitted with a single-exponential model, giving a photodegradation rate constant of k = 0.041 h^{-1} and a half-life of $t_{1/2}$ = 16.75 h (Figure S18). This systematic investigation unequivocally identified the labile nature of the blue-emitting guest as the single point of failure. Crucially, the observation that the **Eu-P6MOF-C1** composite remained unstable underscores a critical insight: the protective confinement offered by the MOF host cannot fully compensate for the profound intrinsic photolability of a guest molecule like C1.

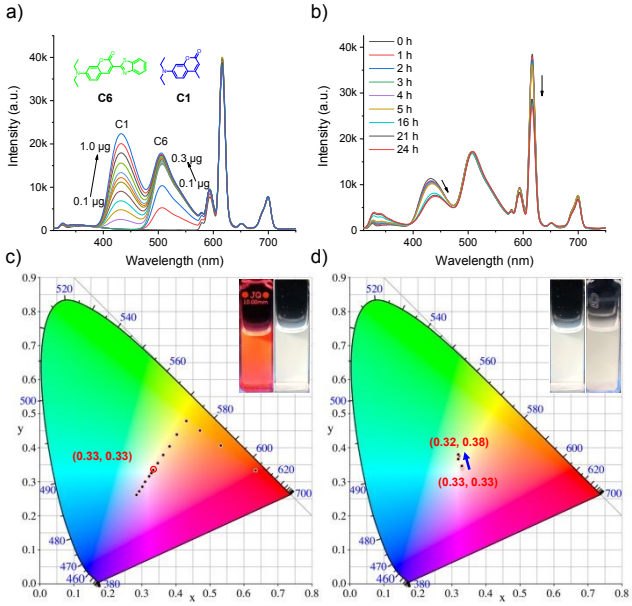

Figure 3. White-light tuning and photostability evaluation of host-guest composites. (a-d) In DMF: (a) Emission spectra demonstrating white-light tuning upon sequential addition of C6 and C1 to **Eu-P6MOF**. (b) Photostability test of the resulting **Eu-P6MOF-C6-C1** composite under prolonged illumination. (c-d) Corresponding CIE 1931 chromaticity diagrams for (a-b), respectively.

Implementing Rational Guest Selection to Forge a Stable White-Emitting System

Guided by this insight, we implemented our rational guest selection strategy by replacing C1 with the highly robust blue emitter, perylene (Figure S19, S20). In DMF, an analogous tuning procedure yielded stable white light (CIE: 0.3283, 0.3348, Figure 4a, 4c and Table S3). Crucially, this new system exhibited exceptional photostability, with negligible coordinate drift under prolonged irradiation, starkly contrasting the C1-based system (Figure 4b, 4d and Table S4). Furthermore, the white-

light emission remained highly stable during storage, with the CIE coordinates changing only slightly from (0.3246, 0.338) to (0.3058, 0.3095) after 197 days (Figure 4e, 4f and Table S5). Powder X-ray diffraction (PXRD) measurements confirmed that the framework structure remained intact (Figure S21). This direct comparison provides a compelling demonstration of how a simple change in guest selection, guided by molecular-level reasoning, can decisively engineer macroscopic stability.

To further examine the generality of the Rational Guest Selection principle, an additional blue-emitting dye with higher intrinsic photostability, 9,10-diphenylanthracene (DPA), was also investigated. The **Eu-P6MOF-C6-DPA** system in DMF similarly produced stable white-light emission and exhibited good photostability, consistent with the proposed design principle. (Figures S22, S23 and Table S6, S7).

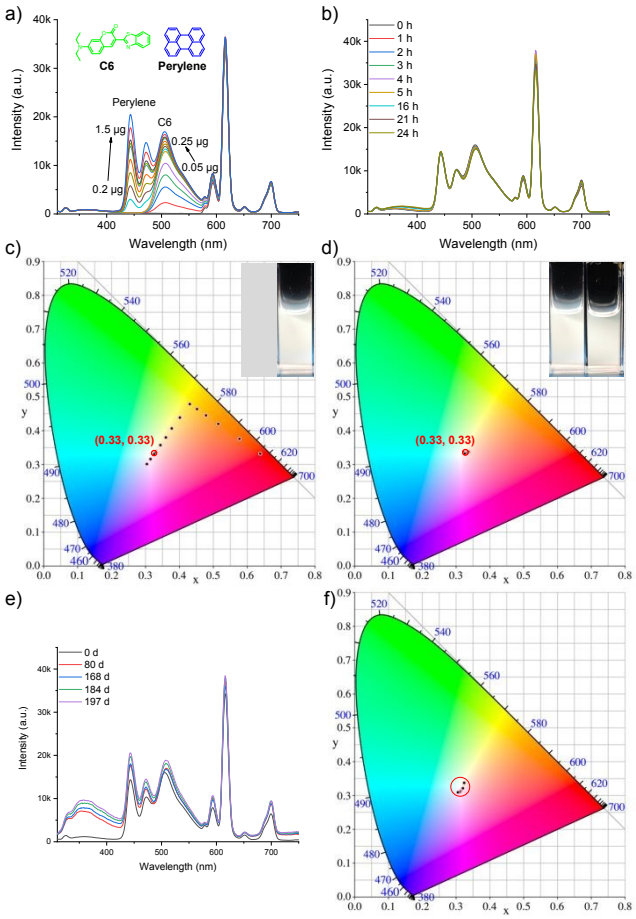

Figure 4. White-light tuning and photostability evaluation of host-guest composites. (a-d) In DMF: (a) Emission spectra demonstrating white-light tuning upon sequential addition of C6 and Perylene to **Eu-P6MOF**. (b) Photostability test of the resulting **Eu-P6MOF-C6-Perylene** composite under prolonged illumination. (c-d) Corresponding CIE 1931 chromaticity diagrams for (a-b), respectively. (e) Photostability of the stable Perylene-based system in DMF after 197 days of daylight exposure. (f) Corresponding CIE 1931 chromaticity diagrams for (e).

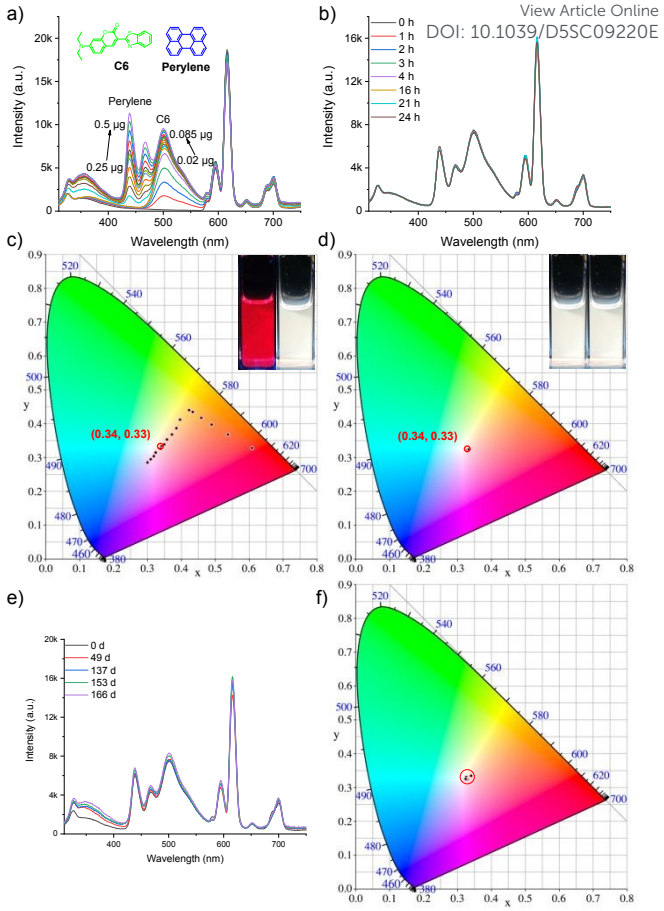

Figure 5. Generalization in ethanol. (a, b) White-light tuning and photostability of the stable **Eu-P6MOF-C6-Perylene** composite. (c-d) Corresponding CIE 1931 chromaticity diagrams for (a-b), respectively. (e) Photostability of the stable Perylene-based system in EtOH after 166 days of daylight exposure. (f) Corresponding CIE 1931 chromaticity diagrams for (e).

Generalization of the Principle in a Green Solvent

The generality of this strategy was further demonstrated in low-toxicity ethanol. To showcase the universality of the principle, we directly employed the stable perylene/C6 pair (Figures S24-S26). Successful white-light generation and exceptional stability were achieved, mirroring the results in DMF. The composite exhibited virtually no change in CIE coordinates after 24 hours of illumination, after 166 days of storage, the CIE coordinates shifted from (0.3404, 0.3342) to (0.3238, 0.3252), with a minimal variation, demonstrating the stability of this system. (Figure 5a-5f, Table S8, S10, S11). In contrast, the C1-based system in ethanol again showed significant chromaticity drift (Figure S27-S29, Table S9, S10), replicating the failure mode observed in DMF. This consistent outcome across different solvent environments conclusively validates rational guest selection as a universal design principle.

Unraveling the Photophysical Mechanism and Quantifying Performance

View Article Online
DOI: 10.1039/D5SC09220F

Time-resolved photoluminescence decays deliver critical insight into the host-guest interactions and the MOF's confinement effect (Figures S30–S53, Table S12). Our proposed mechanism (Figure 6) attributes the observed stability to a synergistic interplay: the Eu^{3+} heavy-atom effect promotes intersystem crossing, while the framework's rigidity severely restricts molecular motion. Crucially, the lifetime data reveal a dual photophysical behavior. The **Eu-P6MOF** host itself exhibits a millisecond-scale lifetime (644.87 μs in DMF) upon excitation at 375 nm with a microsecond lamp, which is a definitive signature of room-temperature phosphorescence (RTP), originating from the ligand-based excited states stabilized by the heavy-atom effect and rigid framework. The lifetime data further suggest that the excited-state relaxation behavior, particularly the contribution of non-radiative decay pathways, is strongly influenced by the guest's intrinsic structural stability. To further probe the role of molecular motion in non-radiative decay, temperature-dependent fluorescence lifetime measurements were conducted (Figures S54–S59, Table S13). Both systems exhibit a gradual decrease in lifetime with increasing temperature (50–100 °C), consistent with thermally activated non-radiative processes. Notably, the C1-based system shows a relatively smaller variation, whereas the perylene-based composite displays a more pronounced temperature dependence, indicating that the excited-state stabilization in the latter is more strongly associated with the MOF confinement effect. The labile C1 molecule retains substantial vibrational freedom that, as mirrored in its nanosecond-scale lifetime, the confinement cannot overcome, resulting in dominant non-radiative decay and rapid photodegradation. Conversely, the structurally rigid perylene dye capitalizes on the MOF's environment, a fact corroborated by its stable excited-state dynamics, which effectively minimizes detrimental processes and ensures a highly efficient radiative pathway. Thus, the MOF host not only provides a protective RTP-active scaffold but also selectively stabilizes guests based on their innate rigidity.

To further examine whether host–guest interaction strength governs the observed stability, binding energy calculations were performed (Figures S60–S63). All calculated binding energies are negative, confirming the thermodynamic feasibility of host–guest complexation in all cases. Notably, although the C1 molecule exhibits a more favorable binding tendency toward the framework, its corresponding composite shows inferior photostability. This apparent discrepancy indicates that binding strength alone does not dictate stability, thereby reinforcing that the suppression of non-radiative decay—primarily governed by the guest's intrinsic structural rigidity and its response to confinement—is the dominant factor.

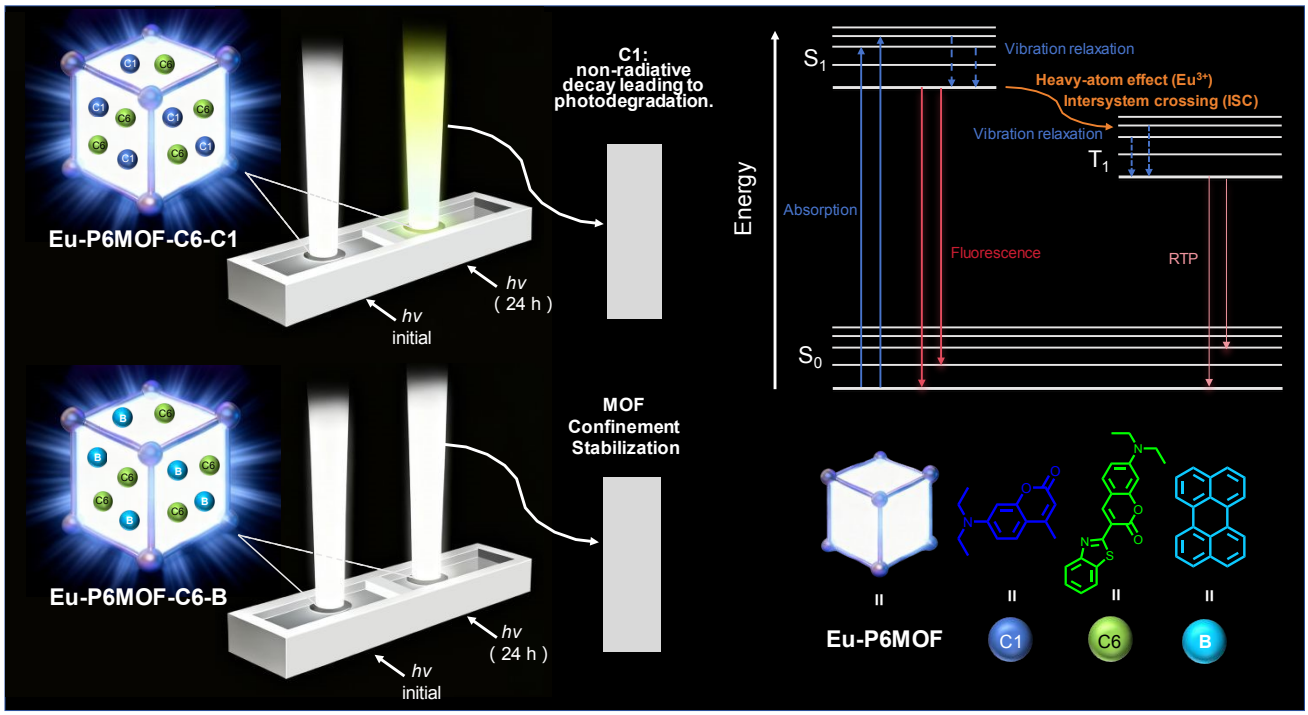

Figure 6. Schematic illustration of the photophysical mechanisms governing stability. In the unstable **Eu-P6MOF-C6-C1** system, the flexible C1 molecule undergoes dominant non-radiative decay, leading to photodegradation. In the stable **Eu-P6MOF-C6-Perylene** system, the synergy between the rigid MOF confinement and the heavy-atom effect from Eu^{3+} ions effectively suppresses the non-radiative decay pathways that lead to photodegradation, thereby locking the perylene dye in a stable, highly emissive state. ISC: intersystem crossing.

View Article Online
DOI: 10.1039/D5SC09220E

ARTICLE

The performance supremacy engineered by rational guest selection is unambiguously quantified by absolute photoluminescence quantum yield (QY) measurements (Figures S64-S89, Table S14). The composite incorporating stable perylene achieved a notable QY of 58.91% in DMF under direct excitation, substantially outperforming the C1-based system (10.90%). Critically, this high efficiency was maintained in the sustainable ethanol solvent, with the perylene-based composite reaching an exceptional QY of 71.8%. This decisive comparison demonstrates that our strategy simultaneously overcomes the stability bottleneck and elevates luminescence efficiency, underscoring a fundamental advantage over conventional design approaches.

Conclusions

In summary, this work establishes Rational Guest Selection as a powerful and universal principle for engineering the operational stability of multi-component luminescent materials. By moving beyond traditional host engineering and proactively prioritizing the intrinsic photostability of emissive guests, we have demonstrated a direct pathway to overcome the longstanding challenge of photodegradation. This research delivers three key advances: (1) the introduction of the first family of lanthanide-pillararene hybrid frameworks (**Eu-P6MOF**) as a versatile host platform; (2) a mechanistic elucidation that the MOF's rigid confinement, synergizing with a heavy-atom effect, suppresses non-radiative decay and molecular pathways to degradation, with efficacy ultimately dictated by the guest's innate structural rigidity; and (3) the validation of a highly generalizable design principle, proven effective across different solvent environments. The " Rational Guest Selection " paradigm is simple, effective, and transformative. It shifts the focus from merely optimizing the host to making informed molecular-level choices at the guest design stage. This principle of prioritizing intrinsic molecular stability opens a new dimension for designing not only durable luminescent materials but also a broad range of host-guest functional systems—from catalysts to sensors—where operational longevity is paramount.

Author contributions

B. Y. conceptualized the ideas and supervised the investigations; L. K. J., Y. Y. C., H. L. and B. L. performed the synthesis, performed X-ray single crystal diffraction, TEM, PXRD and fluorescence experiments; L. K. J., Y. Y. C., H. L., B. L. and B. Y. collected the data; L. K. J. Y. Y. C., H. L., B. L. and B. Y. drew the schematic diagram; L. K. J., G. Y. Y., Z. T. L. and B. Y. analysed the data; B. Y. finished the writing.

Conflicts of interest

There are no conflicts to declare.

Data availability

All characterization data and experimental protocols are provided in this article and the SI Appendix. Crystallographic data have been deposited in the Cambridge Crystallographic Data Centre (CCDC) under accession numbers CCDC: 2499388. These data can be obtained free of charge from the Cambridge Crystallographic Date Centre via www.ccdc.cam.ac.uk/data request/cif. Extra data are available from the corresponding author upon request.

Acknowledgements

We thank the Joint Funds of Provincial Science and Technology Research and Development Program of Henan (Advantageous Discipline Cultivation, Nos. 242301420058) .

Notes and references

1 E. F. Schubert and J. K. Kim, *Science*, 2005, **308**, 1274.
2 S. Reineke, F. Lindner, G. Schwartz, N. Seidler, K. Walzer, B. Lüssem and K. Leo, *Nature*, 2009, **459**, 234.
3 C. C. Lin and R. S. Liu, *J. Phys. Chem. Lett.*, 2011, **2**, 1268.
4 X. Wu, Y. Zhang, K. Takle, O. Bilsel, Z. Li, H. Lee, Z. Zhang, D. Li, W. Fan, C. Duan, E. M. Chan, C. Lois, Y. Xiang and G. Han, *ACS Nano*, 2016, **10**, 1060.
5 H. Furukawa, K. E. Cordova, M. O'Keeffe and O. M. Yaghi, *Science*, 2013, **341**, 1230444.
6 Y. Cui, Y. Yue, G. Qian and B. Chen, *Chem. Rev.*, 2012, **112**, 1126.
7 H. C. Zhou and S. Kitagawa, *Chem. Soc. Rev.*, 2014, **43**, 5415.
8 L. Jiao, J. Y. R. Seow, W. S. Skinner, Z. U. Wang and H. L. Jiang, *Mater. Today*, 2019, **27**, 43.
9 X. M. Tong, J. C. Wang, M. M. Wei, J. W. Qiang, Z. H. Gao, F. Q. Hu and Y. S. Zhao, *Aggregate*, 2025, **6**, e70188.
10 C. Lyu, C. F. Zhao, M. M. Wang, J. W. Li, Z. Z. Cai, X. C. Dou and B. Y. Zu, *Aggregate*, 2025, **6**, e70053.
11 U. Resch-Genger, M. Grabolle, S. Cavaliere-Jaricot, R. Nitschke and T. Nann, *Nat. Methods*, 2008, **5**, 763.
12 L. D. Lavis and R. T. Raines, *ACS Chem. Biol.*, 2008, **3**, 142.
13 C. Würth, M. Grabolle, J. Pauli, M. Spieles and U. Resch-Genger, *Nat. Protoc.*, 2013, **8**, 1535.
14 R. Huang, Z. Yu, Z. Li, X. Lin, J. Hou, Z. Hu and J. Zou, *Coord. Chem. Rev.*, 2025, **526**, 216358.
15 A. J. Howarth, Y. Liu, P. Li, Z. Li, T. C. Wang, J. T. Hupp and O. K. Farha, *Nat. Rev. Mater.*, 2016, **1**, 15018.
16 M. Ding, X. Cai and H. L. Jiang, *Chem. Sci.*, 2019, **10**, 10209.
17 H. Q. Yin and X. B. Yin, *Acc. Chem. Res.*, 2020, **53**, 485.

View Article Online
DOI: 10.1039/D5SC09220E

18 X. Zhang, B. Wang, A. Alsalme, S. Xiang, Z. Zhang and B. Chen, *Coord. Chem. Rev.*, 2020, **423**, 213507.
19 J. Chen, M. Li, R. Sun, Y. Xie, J. R. Reimers and L. Sun, *Adv. Funct. Mater.*, 2024, **34**, 2315276.
20 X. Y. Liu, K. Xing, Y. Li, C. K. Tsung and J. Li, *J. Am. Chem. Soc.*, 2019, **141**, 14807.
21 C. Wang, D. Liu and W. Lin, *J. Am. Chem. Soc.*, 2013, **135**, 13222.
22 Y. Wen, T. Sheng, X. Zhu, C. Zhuo, S. Su, H. Li, S. Hu, Q. L. Zhu and X. Wu, *Adv. Mater.*, 2017, **29**, 1700778.
23 M. Gutiérrez, Y. Zhang and J. C. Tan, *Chem. Rev.*, 2022, **122**, 10438.
24 F. Würthner, C. R. Saha-Möller, B. Fimmel, S. Ogi, P. Leowanawat and D. Schmidt, *Chem. Rev.*, 2016, **116**, 962.
25 S. Cai, H. Shi, D. Tian, H. Ma, Z. Cheng, Q. Wu, M. Gu, L. Huang, Z. An, Q. Peng and W. Huang, *Adv. Funct. Mater.*, 2018, **28**, 1705045.
26 W. Zhao, Z. He and B. Z. Tang, *Nat. Rev. Mater.*, 2020, **5**, 869.
27 M. Xue, Y. Yang, X. Chi, Z. Zhang and F. Huang, *Acc. Chem. Res.*, 2012, **45**, 1294.
28 T. Ogoshi, T. Yamagishi and Y. Nakamoto, *Chem. Rev.*, 2016, **116**, 7937.
29 N. Song, T. Kakuta, T. Yamagishi, Y. W. Yang and T. Ogoshi, *Chem*, 2018, **4**, 2029.
30 W. Si, P. Xin, Z. T. Li and J. L. Hou, *Acc. Chem. Res.*, 2015, **48**, 1612.
31 Y. Wu, L. Shi, L. Xu, J. Ying, X. Miao, B. Hua, Z. Chen, J. L. Sessler and F. Huang, *Nature*, 2025, **640**, 676.
32 N. L. Strutt, D. Fairen-Jimenez, J. Iehl, M. B. Lalonde, R. Q. Snurr, O. K. Farha, J. T. Hupp and J. F. Stoddart, *J. Am. Chem. Soc.*, 2012, **134**, 17436.
33 Y. Wu, M. Tang, Z. Wang, L. Shi, Z. Xiong, Z. Chen, J. L. Sessler and F. Huang, *Nat. Commun.*, 2023, **14**, 4927.
34 C. J. Clarke, W. C. Tu, O. Levers, A. Bröhl and J. P. Hallett, *Chem. Rev.*, 2018, **118**, 747.
35 Z. N. Chen, L. P. Zhang, H. L. Wu, Q. Y. Qi, M. Yan, J. Tian, G. Y. Yang, Z. T. Li and B. Yang, *Chem. Sci.*, 2024, **15**, 13191.
36 M. Y. Zhang, W. L. Yang, L. K. Jing, B. Lv, Z. N. Chen, Q. Y. Qi, J. Tian, G. Y. Yang, Z. T. Li and B. Yang, *Nano Res.*, 2025, **18**, 94907705.
37 B. Lv, Y. Y. Chang and B. Yang, *Adv. Funct. Mater.*, 2025, e16148.

View Article Online
DOI: 10.1039/D5SC09220E

All characterization data and experimental protocols are provided in this article and the SI Appendix. Crystallographic data have been deposited in the Cambridge Crystallographic Data Centre (CCDC) under accession numbers CCDC: 2499388. These data can be obtained free of charge from the Cambridge Crystallographic Date Centre via www.ccdc.cam.ac.uk/data request/cif. Extra data are available from the corresponding author upon request.